Peer-reviewed version available at Bioengineering 2018, 5, 12; doi:10.3390/bioengineering5010012

Article

Delivery of Mesenchymal Stem Cells from Gelatin-Alginate Hydrogels to Stomach Lumen for Treatment of Gastroparesis

Binata Joddar[1,2,*], Nishat Tasnim[1], Vikram Thakur[3], Alok Kumar[1], Richard W. McCallum[4], Munmun Chattopadhyay[3,*]

[1] Inspired Materials & Stem-Cell Based Tissue Engineering Laboratory (IMSTEL), Department of Metallurgical, Materials and Biomedical Engineering, University of Texas at El Paso, 500 W University Avenue, El Paso, TX 79968, USA.
[2] Border Biomedical Research Center, University of Texas at El Paso, 500 W University Avenue, El Paso, TX 79968, USA.
[3] Department of Biomedical Sciences, Center of Emphasis in Diabetes and Metabolism, Texas Tech University Health Sciences Center, 5001 El Paso Drive, El Paso, TX 79905, USA.
[4] Department of Internal Medicine, Paul L. Foster School of Medicine, Texas Tech University Health Sciences Center, 4800 Alberta Avenue, El Paso, TX 79905, USA.
* Corresponding/Senior Author/s: Binata Joddar; bjoddar@utep.edu; Phone: (915) 747-8456, Fax: (915) 747-8036; Munmun Chattopadhyay; munmun.chattopadhyay@ttuhsc.edu; Phone: (915) 215-4170, Fax: (915) 215-8875.

Abstract: Gastroparesis (GP) is associated with depletion of interstitial cells of Cajal (ICC) and enteric neurons, which leads to pyloric dysfunction followed by severe nausea, vomiting and delayed gastric-emptying. Regenerating these fundamental structures with stem cell therapy, would be helpful to restore gastric function in GP. Mesenchymal stem cells (MSC) have been successfully used in animal models of other gastrointestinal (GI) diseases including colitis. However, no study has been performed with these cells on GP animals. In this study, we explored if mouse MSC can be delivered from a hydrogel-scaffold to the luminal surfaces of GP mice stomach. Mouse MSC was seeded atop alginate-gelatin, coated with poly-L-lysine. These cell-gel constructs were placed atop stomach explants facing the luminal side. MSC grew uniformly all across the gel surface within 48 hr. When placed atop the lumen of the stomach, MSC migrated from the gels to the tissues as confirmed by positive staining with Vimentin and N-cadherin. The feasibility of transplanting a cell-gel construct to deliver stem cells in the stomach wall was successfully shown in a mice GP model, thereby making a significant advance towards envisioning the transplantation of an entire tissue-engineered 'gastric patch' or 'microgels' with stem cells, and growth factors.

Keywords: tissue engineering; lumen; stem cells; interstitial cells of Cajal; hydrogel scaffolds

1. Introduction

Gastroparesis (GP), a condition affecting almost 10 million individuals in the United States (US), is a common gastrointestinal (GI) motility disorder characterized by delayed gastric emptying without any mechanical obstruction [1]. Studies in animal models, as well as patients with GP, have revealed depletion or ultrastructural changes of Interstitial cells of Cajal (ICC) in the gastric tissue [1]. ICC function as the pacemakers of the GI tract and are involved in the transmission of the neuronal signaling to the smooth muscles. Therefore their existence in the stomach wall is of prime importance for their properties of slow-wave generation and propagation which allows for the movement of food through the digestive canal [1]. Loss of ICC is believed to result in conditions of gastroparesis and may even lead to gastric cancer [2, 3]. GP is also associated with the depletion of enteric neurons including nitric oxide synthase (nNOS) expressing neurons [4]. The depletion of nNOS results in

pyloric dysfunction and delayed gastric emptying [4]. Treatment options are limited, with the most common treatment being surgical resection of the stomach or gastrectomy, however, post gastrectomy many patients suffer various unwanted after-effects including bloating, loss of appetite and malnutrition [1]. Regenerative stem cell therapies, based on principles of tissue engineering, have been proposed as a therapeutic possibility to restore the levels of depleted ICC and the normal physiological functions of the stomach wall [5]. Previous studies adopted an acellular materials-based approach using collagen-based scaffolds, to induce new tissue growth within the host [5-7], but these efforts failed to restore function to the diseased stomach wall. Other cell-based approaches, centered on building stomach-epithelium-organoid units for overcoming the difficulties of isolating and culturing gastric epithelial cells, in-vitro [5]. These efforts lead to the development of vascularized tissue with a neo-mucosa and also indicated the presence of a smooth muscle layer and gastric epithelium, as well as the existence of parietal cells of the stomach mucosa, post-implantation [5]. However, the isolation of stomach-epithelium-organoid units is extremely challenging [5]. We conceived an alternative, simpler and more feasible technique of delivering cells from hydrogel scaffolds to the stomach tissue lumen in-vitro such that, if successful this approach can then be translated in-vivo. In this study, mouse Mesenchymal Stem Cells (MSC) were seeded atop an alginate-gelatin scaffold for placing on luminal surfaces of mouse stomach explants, in-vitro. The possibility of using bone marrow- and other non-gut-derived murine MSC for in-vivo immunosuppression after allogeneic transplantation, is well established [8]. We hypothesized that the mouse MSC would adhere, proliferate within the alginate-gelatin scaffold and upon being placed atop the stomach tissue would migrate from the gels to the actual tissue sections. The results yielded from this work will lead us to our long-term goal, to deliver MSC or other stem cells such as induced pluripotent stem cells (iPSC), from a bioengineered scaffold to the host stomach wall, to help restore the depleted levels of ICC and lead to regeneration of smooth muscle tissue leading to overall physiological improvement of the stomach wall. Regeneration of ICC and nNOS expressing neurons in the stomach wall would restore gastric function in GP [9]. Stem cell therapy is considered as a potential treatment for GP [10]. However, studies on this novel treatment strategy are scarce majorly because of technological limitations, including short survival of the stem cells and their insufficient adhesion and migration as well as insufficient regeneration of the target cells which are affected during pathological conditions [11]. MSCs have been successfully used in animal models of GI diseases including colitis and could regenerate enteric neurons and glia [10]. However, no previous study has been performed with these cells on GP models. Our pilot study, for the first time, will highlight the feasibility of delivering stem cells via a hydrogel scaffold, to stomach tissues in-vitro. In future, we aim to synthesize microgels using these materials, for delivering stem cells and other regenerative factors via laparoscopy, to the GP stomach lumen in the clinic.

2. Materials and Methods

2.1. Materials for fabrication of the alginate-gelatin hydrogel

Sodium alginate (Cat. No. 218295) and type-A gelatin (Cat. No. 901771) was obtained from MP Biomedicals (Strasbourg, France). 1-ethyl-3-(-3-dimethylaminopropyl) carbodiimide hydrochloride (EDC, Cat. No. 22980) and N-hydroxysuccinimide (NHS, Cat. No. 24500) were purchased from Thermo Scientific (Rockford, IL, USA). Calcium chloride (Cat. No. C79-500) and 1X Phosphate Buffered Saline (PBS) was purchased from Fisher Chemicals (Fair Lawn, NJ, USA). The method used for hydrogel synthesis was adopted from previous studies carried out by Wang et al. [12] and Hernandez et al. [13]. The hydrogel was prepared by the crosslinking of an alginate and gelatin mixture with 1-ethyl-3-(3-dimethylaminopropyl) carbodiimide (EDC) and N-hydroxy-succinimide (NHS), followed by calcium chloride (CaCl2). During hydrogel synthesis, EDC was used to activate the carboxyl groups of alginate to form active ester groups, followed by NHS bonding with alginate due to the replacement of EDC to improve the efficiency of amine reaction [14, 15]. Briefly in 10 mL distilled water gelatin and sodium alginate, 200 mg of each were added and stirred (at room temperature for 15 min at 100 rpm). After this, 25 mg EDC was added (stirred at room temperature

for 10 min), followed by addition of 15 mg NHS (stirring for another 5 min at room temperature) to make the gel-like mixture. For sterilization, this gel mixture was irradiated with UV light for 30 min. After sterilization, the viscous mixture was poured into a 100 mm petri dish and tapped gently to make a smooth layer with a flat surface. After this 1M CaCl2 was added on the surface of the gelatin-alginate mixture and allowed to react for 15-20 mins. Then, the CaCl2 solution was removed from the surface of the formed gel and the petri dish with gel washed with 1X PBS, thrice.

2.2. Materials characterization and analysis of the hydrogel

For all characterization, gels cast without cells were used. All samples were present in triplicate unless otherwise mentioned.

a) X-Ray Diffraction Analysis (XRD)- For the phase analysis, the gel samples were frozen and lyophilized prior to XRD (D8 Discover, Bruker's diffractometer, Karlsruhe, Germany). XRD was carried out at 40 kV voltage and 40 mA current with CuKα wavelength (1.54056 Å) and 2θ ranges from 10° to 50° at a scanning rate of 3°/min with a step size of 0.1°.

b) Fourier transform infrared spectroscopy (FTIR)- FTIR was used to reveal information about the molecular structure of the crosslinked gel sheet. Attenuated total reflectance (ATR)-FTIR spectra of a representative gel sample was acquired using a Perkin-Elmer, Spectrum 100, Universal ATR Sampling Accessory within the range of 700–3700 cm−1 in transmittance mode. Spectral manipulations were performed using the spectral analysis software GRAMS/32 (Galactic Industries Corp., Salem, NH, USA). External reflection FTIR was recorded on a Specac grazing angle accessory using an s-polarized beam at an angle of incidence of 40° and a mercury cadmium telluride (MCT/A) detector. A piranha-treated silicon wafer was used as the background.

c) Scanning Electron Microscopy (SEM)- SEM was operated in secondary electron mode for the analysis of the morphology of the gel samples. Samples were visualized using SEM (S-4800, Hitachi, Japan) at voltages of 8 kV. Prior to SEM, to minimize charging during observation, samples were coated using Graphite spray (Electron Microscopy Sciences, Hatfield, PA).

d) Swelling and Degradation- To account for the hydration parameters of the alginate-gelatin gels leading to swelling, gels were allowed to swell to equilibrium for 5 days in Simulated Gastric Fluid (Ricca Chemical, Arlington, TX) at 25°C, to identify the time point when the weight of the gels was found to be constant, or the final swelling degree was attained. Disc-shaped punch out samples (8-mm biopsy punch) were lyophilized to reveal their dry weight (W0), prior to being exposed to the aqueous media. The gels were then allowed to swell during which they were taken out at regular intervals of 1 day, the excess surface liquid was absorbed using blotting paper and the gels were weighed (Wt). The swelling ratio was calculated using the following equation (1), where Ds was the degree of swelling, W0 and Wt were the weights of the samples in the dry and swollen states respectively [16].

$$Ds=(Wt-W0)/W0 \quad (1)$$

e) Mechanical testing- All mechanical testing was done using an ElectroForce 5100 Biodynamics Test Instrument from ElectroForce Systems group (Bose Corporation, Framingham, MA) [16]. For testing, a dog-bone sample was cut using a mold on the alginate-gelatin hydrogels and carefully mounted between pressure grips, as done before [16]. Mounted specimens had an estimated cross-sectional area of 5 mm and a gauge length of 15 mm, and were maintained in CaCl2 to prevent aging of the hydrogels [16]. The mechanical properties of the hydrogels were evaluated by measuring stress-strain curves via uniaxial compression at the rate of 1 mm min−1 until they were completely fractured [16]. The elastic modulus of each sample was calculated from the slope of the stress-strain linear curves generated by the data [16]. Data are expressed as the mean ± standard deviation.

Peer-reviewed version available at Bioengineering 2018, 5, 12; doi:10.3390/bioengineering5010012

2.3. Cell Culture

Mouse MSC (Strain C57BL/6 Mouse Mesenchymal Stem Cells), basal culture medium and growth supplements were obtained from Cyagen (Santa Clara, CA). A green fluorescent dye (PKH67, Cat. No. MINI67) for the pre-staining of cells prior to cell culture was purchased from the Sigma Aldrich (St. Louis, MO, USA). 1× Cell Dissociation Medium (0.25%Trypsin supplemented with 2.21 mM EDTA, Cat. No. 25-053-Cl) and 1X PBS (Cat. No. K812-500) were purchased from Mediatech, Corning (Masassas, VA, USA) and Amresco (Solon, OH, USA), respectively. Prior to being used for cell culture, the alginate-gelatin scaffolds were coated using poly-L-lysine (Sigma-Aldrich) and UV sterilized again (~15 min) [13]. For cell seeding atop the scaffolds, Mouse MSCs were thawed and seeded in a 25 cm2 tissue culture flask containing 5 ml tissue culture medium (MUXES-90011) obtained from (Cyagen) and supplemented with 10% FBS, Glutamine, Penicillin-Streptomycin, Non-Essential amino acids, LIF and 2-mercaptoethanol. Passaged and stabilized mouse MSC was trypsinized using 0.25% trypsin-EDTA and cells pre-stained with PKH67 as per manufacturer's protocols. These pre-stained cells were centrifuged to remove the cell-suspension media and were seeded atop these scaffolds in a density of 50,000 cells/ml.

2.4. In-vitro transplants of cell-gel constructs atop stomach tissue

All institutional and national guidelines for the care and use of laboratory animals were followed and approved by the appropriate institutional committees at Texas Tech University Health Sciences Center (TTUHSC). C57BL/6 mice were euthanized and their stomach was harvested. The harvested stomach was drained of its contents and cleaned with 0.9% saline wash (BD Scientific, San Jose, CA). The stomach was then transferred to a cell culture dish (60X15 mm) containing the growth medium (DMEM 10566-016) supplemented with GlutaMax 1, 10% fetal bovine serum, 1% non-essential amino acids, 1% Sodium Pyruvate, 1% Penicillin-Streptomycin (all sourced from Gibco), 50 mg/ml Gentamicin (Sigma-Aldrich) and 10ug/ml Insulin-Transferrin-Selenium-X (Sigma-Aldrich). The stomach explants were left overnight (24 hr) in this medium [17]. In the meantime, MSCs were dispersed by trypsin-EDTA and were reseeded on the hydrogel sheet until a monolayer of MSC was observed. A piece of the hydrogel sheet (~ 5-6cm2) with the monolayer of MSC was cut carefully. This piece of hydrogel was then placed on to the luminal side of stomach. The stomach along with the hydrogel was kept incubating (37°C, 5% CO2) for another 48 hrs.

2.5. Probing the migration of MSC from gels into tissue (Immunocytochemistry)

Chemicals used in this step included an optimum cutting temperature (O.C.T) compound (Embedding medium, Fisher HealthCare, PA), 4% paraformaldehyde (Sigma-Aldrich) and Fluoromount G (Electron Microscopy Sciences, Fort Washington, PA) for mounting the tissue sections. Antibodies used were anti-Vimentin (1:400; Cell Signaling), anti-N-Cadherin (1:400 Cell Signaling, USA) and Alexa Fluor 594 goat anti-rabbit IgG (1:1000, Molecular Probe, Eugene, OR). As a counterstain DAPI (Vector Labs, CA, USA) was used. After 48 hrs, the medium was removed from the wells and the hydrogel sheet along with the stomach was washed once with PBS, and then embedded in the O.C.T. Compound (embedding medium, Fisher HealthCare) for frozen tissue sectioning. The tissue was cryo-sectioned at 5 μm and collected on gelatin-coated slides, fixed with 4% paraformaldehyde for 20 min, washed 3X with PBS, and incubated with blocking solution (PBS with 1% normal goat serum and 0.3% Triton X-100) for 1 hr, then washed once. The stomach sections were then incubated with anti-vimentin (1:400; Cell Signaling) or anti-N-cadherin (1:400 Cell Signaling, USA) for 2 hr at room temperature and washed thrice with 1X PBS followed by incubation in the secondary fluorescent antibody, Alexa Fluor 594 goat anti-rabbit IgG (1:1000, Molecular Probe, Eugene, OR) for 1 hr at room temperature. The specimens were then washed 3X with PBS followed by DAPI staining (1:50,000). The specimens were again washed 3X with PBS and mounted with water-based Fluoromount G (Electron Microscopy Sciences, Fort Washington, PA). Digitized images of immunostained sections were captured with a Nikon NiE fluorescent microscope (Nikon, USA), and analyzed using the NiS elements computer-based image analysis system (Nikon, USA). The

intensity of the immunostained stem cells in the stomach tissue was determined using an image analysis software, Image J (NIH). Three cross-sections of the tissues were evaluated in each case.

3. Results

3.1. Phase identification and chemical characterization

The crystalline phases of the gelatin-alginate hydrogel sheet about 2-4 mm thick (Figure 1A) were determined by X-ray powder diffraction after being frozen and lyophilized. The X-ray diffraction (XRD) patterns of alginate-gelatin are shown in Figure 1B. The diffraction peak for sodium alginate at 2θ = 38.40 appeared with high-intensity in the spectra with another high-intensity peak appearing at 2θ = 43.930 which suggested that the composition became crystalline from semi-crystalline nature of alginate [18]. Some of the other characteristic peaks for sodium alginate were observed in the scaffold with a slight shift in 2θ values (28.96° to 31.74° and 36.64° to 39.62°) [18]. The absence of other lower angle diffraction peaks of alginate (at 13.570 and 22.750 [19]) and the characteristic peak of gelatin (at 2θ = 20.90 for triple-helical crystalline structure [20]) show the strong interactions between alginate and gelatin in the scaffold and more crystalline characteristics [21]. The crystalline nature indicates that the gelatin was modified with alginate after being crosslinked which can provide better tissue culture properties for the scaffold, such as cell adhesion, hydrophilicity, increased biomechanical functionality, and biodegradation rate [22]. The components of the gelatin-alginate scaffold were determined by FTIR spectroscopy after being frozen and lyophilized. There were four characteristic peaks of the scaffold shown in Figure 1C. The characteristic peaks appeared at 3430 (–OH stretching), 1616 (–CO– stretching),1417 (–COOH stretching), 1092 (C–O stretching) and 1030 cm-1 (C–O–C stretching), which are characterized by saccharide structure of alginate [23]. The characteristic peaks of gelatin protein structure (at 1630 and 1543 cm-1) assigned to the N–H stretching vibration peaks for amide I and amide II are absent in the spectra proving the involvement of this group in the crosslinking reaction which is in agreement with the XRD results [21, 24].

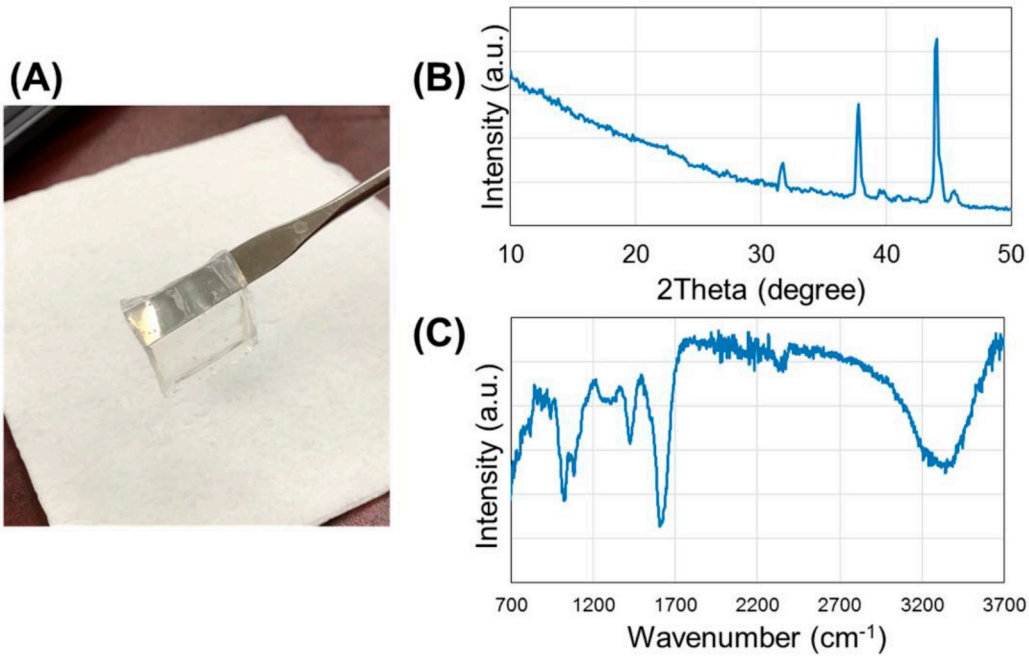

Figure 1. (A) Hydrogel sheet. (B) XRD spectra of the hydrogel. (C) FTIR spectra of the hydrogel.

3.2. Microstructure Imaging

SEM images revealed a highly porous structure of the hydrogel with an average pore size of 1.05 ± 0.37 μm and apparent porosity of 9% (Figure 2A). The pores appeared to be homogenously

Peer-reviewed version available at Bioengineering 2018, 5, 12; doi:10.3390/bioengineering5010012

networked and distributed throughout the entire structure (Figure 2A). This indicated that this structure would allow enhanced circulation of nutrients and media, and would be stable in-vivo.

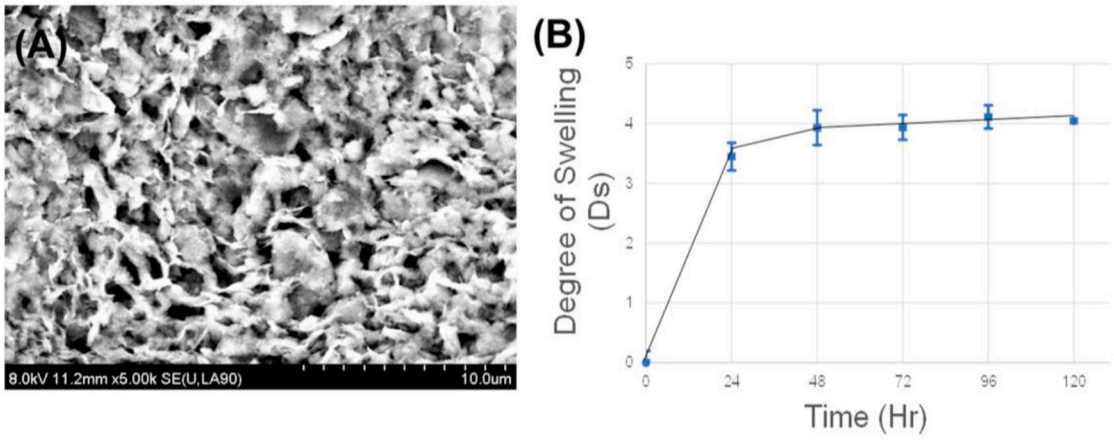

Figure 2. (A) SEM image of the hydrogel. (B) Swelling and Degradation analysis.

3.3. In-Vitro Stability

Swelling and Degradation analysis performed using simulated gastric fluid, showed maximum swelling after 24 hr, following which the gels were seen to attain equilibrium with no evidence of degradation (Figure 2B). Thus the cell-gel constructs are expected to maintain their structural fidelity when implanted in-vivo for a sustainably long period of time even when exposed to the harsh acidic environment of the stomach.

3.4. Mechanical Stiffness

Average elastic modulus of the gels was about 117 ± 23 kPa, which implied that these hydrogels would maintain structural fidelity, in-vivo (Figure 3) as they appeared to be stiffer than other hydrogels commonly used for tissue engineering [16, 25] and transplant applications [26, 27].

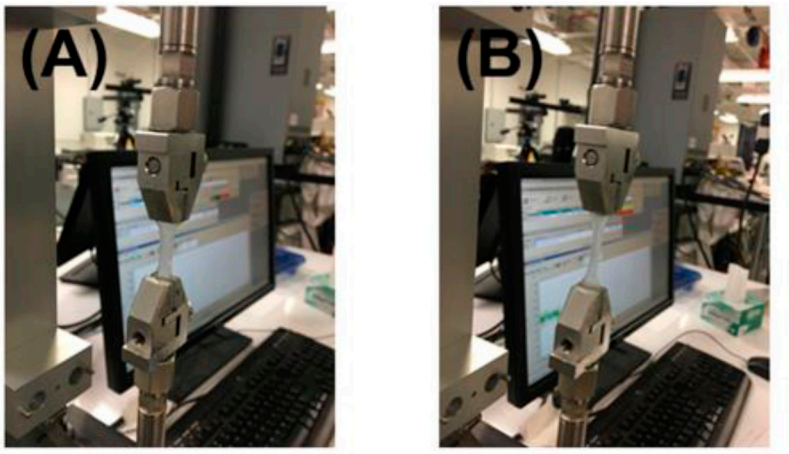

Figure 3. Mechanical testing to measure stiffness moduli of the hydrogels. Shown in (A) is the gels during the beginning of the experiment. In (B) the load is being applied and the gels appear stretched.

3.5. Biocompatibility

The in-vitro passaged and stabilized MSC (~6th passage) were seeded atop these scaffolds in a density of 50,000 cells/ml. These cell-gel sheets were cultured in complete growth medium for at least

48 hr, following which they were analyzed (Figure 4). Mouse MSC grew uniformly across the entire surface of the gels (Figure 4). However, when a z-scan was conducted over the entire thickness of the cell-gel constructs, maximum cell density was noted in the middle of the constructs (Supplementary Figure 1). This issue can be overcome using a cell bioprinting approach wherein a homogenous layer-by-layer cell density can be easily achieved [28]. Only viable cell-gel constructs were placed atop luminal surfaces of mouse stomach tissue explants.

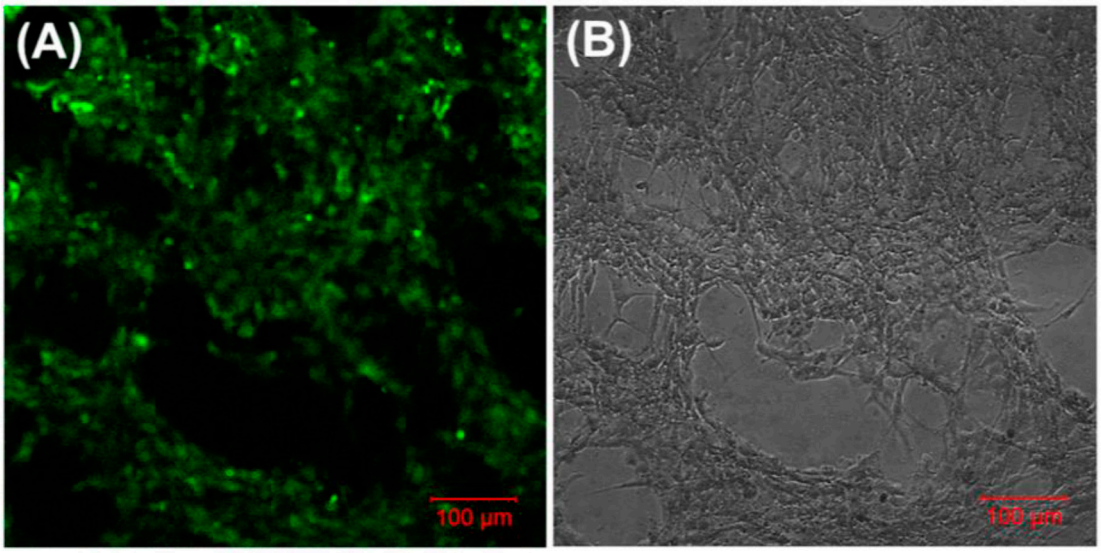

Figure 4. Cyto-compatibility of the poly-L-lysine coated hydrogels. Shown in (A) is mouse mesenchymal stem cells (MSC), pre-stained with PKH-67, growing uniformly across the gel. In (B) a brightfield image of the same is shown.

3.6. Delivery of mouse MSC from gels to stomach tissue

MSC migration within the mouse stomach was probed using antibodies against Vimentin and N-Cadherin, both of which are commonly used markers for stem cells [29]. Interestingly, mouse stomachs that received cell-gel constructs showed the presence of cells that stained positive using both markers, Vimentin (Figure 5A) and N-Cadherin (Figure 5B, during processing the gel got detached from the stomach tissue section). Control stomach explants those of which received only gels or none did not reveal such results. This proves that MSC can be successfully delivered from the gels to the stomach tissue explants and the delivered cells were able to penetrate some substantial distance within the width of the stomach tissue explants used for the experiments.

Peer-reviewed version available at Bioengineering 2018, 5, 12; doi:10.3390/bioengineering5010012

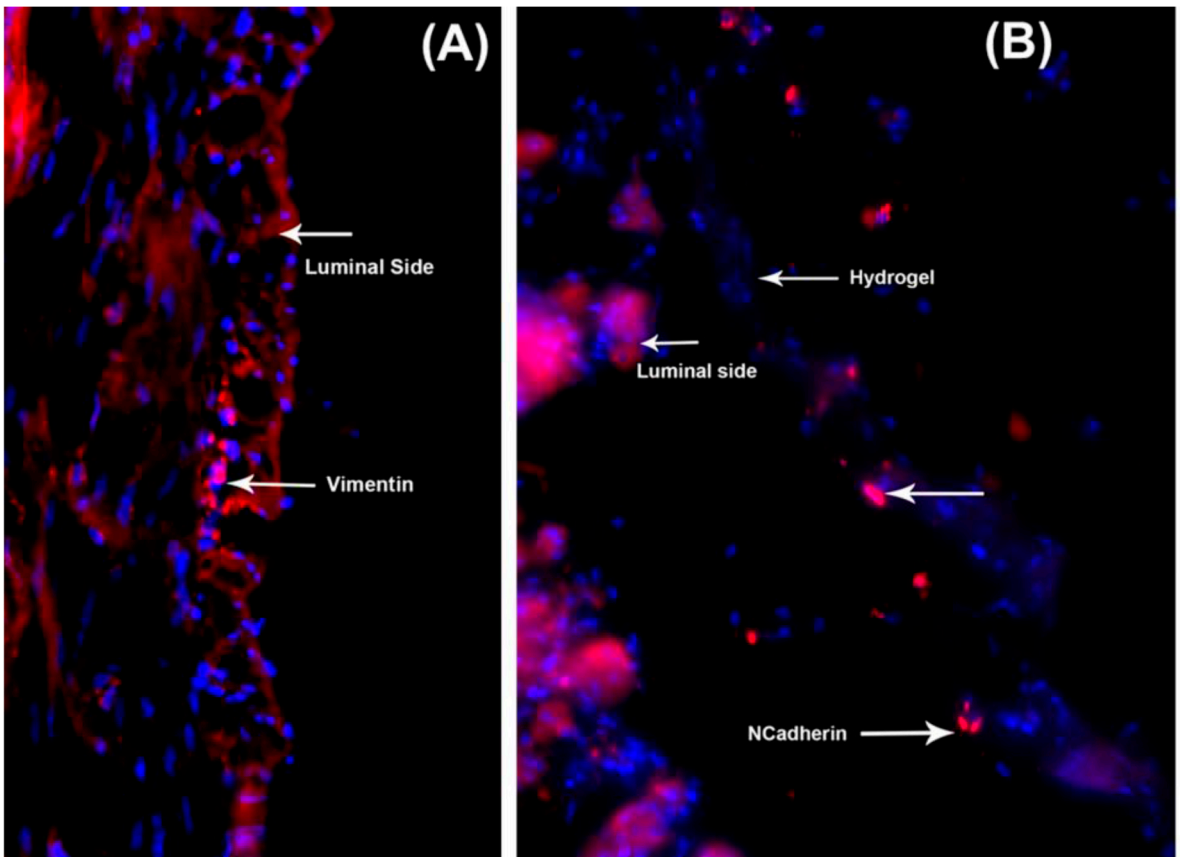

Figure 5. When the mouse MSC seeded gels were placed atop the stomach lumen, the cells migrated from the gels to the luminal tissues as shown by positively stained cells for the stem cell markers, (A) Vimentin and (B) N-Cadherin.

4. Discussion

Loss of ICC cells might be an underlying cause for the development of gastroparesis leading to symptoms such as nausea, vomiting, early satiety, postprandial fullness, bloating, and abdominal pain [1]. Because of limited pharmacological options, surgery including gastric resections has been required with accompanying degrees of morbidity [1]. The limited capacity for food intake after this procedure creates a need for regenerating the stomach [2]. Therefore using principles of tissue engineering, including isolated cells combined with appropriate biomaterials can lead to the formation of a tissue-engineered stomach in-vivo [2]. Cell-based approaches utilizing gastric-epithelial-organoid units seeded on polymeric scaffolds, have been successful in stomach wall repair [2]. These results along with more recent reports [2, 30] emphasized the need for cell-based therapies for stomach tissue engineering and may improve our understanding of the beneficial effect of ICC by regenerative stem cell-based therapies in gastrointestinal complications of diabetes. However, the isolation of specialized units such as the gastric-epithelial-organoid units is technically challenging [2]. Therefore, a much more feasible alternative would be to deliver stem cells via a biomaterial scaffold, for regenerating the stomach wall [8, 10, 31, 32]. Recently, it was shown that gastric stem cells isolated from younger mice when transplanted into sites of injury within the stomachs of older mice, resulted in accelerated repair [33]. This study, in addition to existing literature, highlights the benefits of stem cell transplantation as a glimpse into future treatment strategies for the healing of the motility compromised stomach [2, 5-7, 32-34]. Our study demonstrated that MSC cells can be delivered via an alginate-gelatin scaffold to stomach tissue explants in-vitro.

The possibility of using bone marrow- and other non-gut-derived murine MSC for in-vivo immunosuppression after allogeneic transplantation, is well established [8]. ICC originates from

mesenchymal precursors [35] and a number of animal studies have revealed the plasticity and regenerative capacity of ICC in neonatal and adult ICC-damage models wherein it was demonstrated that the role of stem cells is particularly prevalent [36]. From recent observations that bone-marrow-derived (BM) mesenchymal stem cells are capable of differentiating into osteoblasts, adipocytes, chondrocytes, and myocytes [37]; there is a strong possibility that BM-derived stem cells could also differentiate into ICC. Earlier it has been demonstrated that allotransplantation of ICC into the myenteric plexus of the small intestine successfully induced distinct Kit+- congenitally deficient in myenteric ICC (ICC-MY) networks and rhythmic pacemaker activity [38]. Recently, a group performed BM transplantations to W/WV mutant mice (congenitally deficient in myenteric ICC; ICC-MY) through a similar method to that employed in clinical circumstance [39]. Despite successful colonization, this method is not clinically feasible, owing to lack of clinical experience of its administration and these BM cannot develop into intact and functionally mature ICC under current conditions [38]. Clinically, BM transplantation still presents an extremely high risk of life-threatening complications [38]. Our study shows a prospect of recovery of damaged or interrupted ICC networks using this method. Nevertheless, this study may signify a substantial first step towards an innovative remedial cure for debilitating GI motility disorders.

Our study demonstrated that MSC cells can be delivered via an alginate-gelatin scaffold to stomach tissue explants in-vitro. The possibility of using bone marrow- and other non-gut-derived murine MSC for in-vivo immunosuppression after allogeneic transplantation, is well established [8]. MSC, when cultured in direct contact with other differentiated cell types or their cell-secreted ECM can differentiate into the latter cell type [40]. We envision that if we could possibly deliver MSC via biomaterial scaffolds to the stomach in-vivo, we can then test their ability to restore levels of not only ICC but also nNOS expressing enteric neurons and heal the diseased stomach wall, in the future. In this study, we observed that the MSC cells penetrated through the epithelium of the lumen into the intra-muscular ICC region of the explant of the mouse stomach.

Alginate-based biomaterials are extremely biocompatible and have been utilized as drug delivery systems and cell carriers for tissue engineering [41]. Tuning the basic structure and properties of alginate such as biodegradability, stiffness, gelation and cell affinity can be achieved through combination with other biomaterials, immobilization of specific ligands such as peptide and sugar molecules, and physical or chemical crosslinking [41]. On the other hand, Gelatin is favored in cell culture on account of its biodegradability, biocompatibility in-vivo due to the presence of an RGD-(Arg-Gly-Asp)-sequence [42] and its commercial availability at low cost [43]. When combined in a single scaffold, alginate-gelatin hydrogels can confer both biocompatibility and mechanical rigidity at the same time and are thus popular candidates for tissue engineering applications [44]. Alginate gels can also be engineered as microgels [45, 46], leaving open the possibility of being able to deliver stem cells encapsulated in such vehicles for treatment of GP, in future.

While studies have reported the isolation of stomach epithelium organoid units for tissue engineering of the stomach [2, 5], our approach of delivering isolated stem cells from a scaffold is unique and poses as a simpler and feasible alternative. Delivering stem cells for tissue engineered of the stomach has already proven to be promising [47]. Further, if we incorporate the possibility of 3D bioprinting of layer-by-layer of such scaffolds with cells, higher cell density for delivery can be achieved along with potent growth factors that can be delivered along with the cells for promoting their differentiation into ICC or enteric neurons.

5. Conclusions

The results from this study imply that stem cells such as MSC can be delivered from a biomaterial scaffold to stomach tissues and this approach may be applied in-vivo to help restore gastric function in GP. Thus in future, we hope to fabricate and characterize a tissue-engineered ‘gastric patch’ by 3D bioprinting of MSC-gel constructs containing selected growth factors, to assess the

outcomes of grafting the 'gastric patch' onto the luminal surfaces of diabetic gastroparesis stomach wall in-vivo, including the survival, adhesion and proliferation rates of the MSC, the regeneration of ICC, enteric neurons and other physiological improvements in the stomach wall.

The successful outcomes from this study are particularly significant in its ability to potentially study and impact other gastric pathologies as well. Besides, the cell-gel therapy can be administered to the stomach/GI tract in-vivo during the course of a routine endoscopy procedure in humans, in the future as an envisioned and ideal clinical translation.

Supplementary Materials: Figure S1: Confocal Imaging of cells in gels counterstained for a. Actin, b. DAPI (nucleus) and c. merged (actin and DAPI). In d. Shown is a z-scan where maximum cell density is detected at the center of the gel.

Acknowledgments: B.J acknowledges NIH BUILD Pilot 8UL1GM118970-02 and NIH 1SC2HL134642-01 for funding support and the NSF-PREM program (DMR 1205302) for materials and supplies. N.T acknowledges the Anita Mochen Loya fellowship at UTEP. The authors also acknowledge the use of the Core Facility at Border Biomedical Research Consortium at UTEP supported by NIH-NIMHD-RCMI Grant No. 2G12MD007592. BJ and MC acknowledge the TTUHSC mini seed grant # 183306-533312-20 for funding the animal studies and required materials and supplies. The authors acknowledge help received from Ms. Lola Norton in facilitating the transfer of supplies and materials between UTEP and TTUHSC.

Author Contributions: BJ, MC, and RMC conceived the overall idea of this study. BJ and MC wrote and edited the manuscript, along with inputs from the rest. NT and VT performed the experiments repeatedly, gathered data and made the final figures, as reported in the manuscript. AK optimized the method for making the gels, did the initial cell culture experiments and the mechanical testing and analysis.

Conflicts of Interest: The authors declare no conflict of interest.

References

1. Mohammad, B., et al., *Is Interstitial Cells of Cajal-opathy Present in Gastroparesis?* J Neurogastroenterol Motil, 2015. **21**(4): p. 486-493.
2. Maemura, T., M. Shin, and M. Kinoshita, *Tissue engineering of the stomach.* J Surg Res, 2013. **183**(1): p. 285-95.
3. Zheng, H., et al., *Is gastrointestinal dysfunction induced by gastric cancer peritoneal metastasis relevant to impairment of interstitial cells of Cajal?* Clin Exp Metastasis, 2011. **28**(3): p. 291-9.
4. Lu, H.-L., et al., *Gastric nNOS reduction accompanied by natriuretic peptides signaling pathway upregulation in diabetic mice.* World Journal of Gastroenterology : WJG, 2014. **20**(16): p. 4626-4635.
5. Maemura, T., et al., *Initial assessment of a tissue engineered stomach derived from syngeneic donors in a rat model.* Asaio j, 2004. **50**(5): p. 468-72.
6. Araki, M., et al., *Development of a new tissue-engineered sheet for reconstruction of the stomach.* Artif Organs, 2009. **33**(10): p. 818-26.
7. Hori, Y., et al., *Functional Analysis of the Tissue-Engineered Stomach Wall.* Artificial Organs, 2002. **26**(10): p. 868-872.
8. Dave, M., et al., *Stem cells for murine interstitial cells of Cajal suppress cellular immunity and colitis via prostaglandin E(2) secretion.* Gastroenterology, 2015. **148**(5): p. 978-990.
9. Zhou, Y., et al., *Heparin-binding EGF-like growth factor promotes neuronal nitric oxide synthase expression and protects the enteric nervous system after necrotizing enterocolitis.* Pediatr Res, 2017. **82**(3): p. 490-500.
10. Yang, J., et al., *Heparin-binding epidermal growth factor-like growth factor and mesenchymal stem cells act synergistically to prevent experimental necrotizing enterocolitis.* J Am Coll Surg, 2012. **215**(4): p. 534-45.
11. Orlic, D., *Stem cell repair in ischemic heart disease: an experimental model.* Int J Hematol, 2002. **76 Suppl 1**: p. 144-5.

12. Wang, K., K.C. Nune, and R.D. Misra, *The functional response of alginate-gelatin-nanocrystalline cellulose injectable hydrogels toward delivery of cells and bioactive molecules.* Acta Biomater, 2016. **36**: p. 143-51.
13. Hernandez, I., A. Kumar, and B. Joddar, *A Bioactive Hydrogel and 3D Printed Polycaprolactone System for Bone Tissue Engineering.* Gels, 2017. **3**(3): p. 26.
14. Kuijpers, A.J., et al., *Cross-linking and characterisation of gelatin matrices for biomedical applications.* J Biomater Sci Polym Ed, 2000. **11**(3): p. 225-43.
15. Kuijpers, A.J., et al., *Characterization of the Network Structure of Carbodiimide Cross-Linked Gelatin Gels.* Macromolecules, 1999. **32**(10): p. 3325-3333.
16. Joddar, B., et al., *Development of functionalized multi-walled carbon-nanotube-based alginate hydrogels for enabling biomimetic technologies.* Scientific Reports, 2016. **6**: p. 32456.
17. Vadstrup, K., et al., *Validation and Optimization of an Ex Vivo Assay of Intestinal Mucosal Biopsies in Crohn's Disease: Reflects Inflammation and Drug Effects.* PLOS ONE, 2016. **11**(5): p. e0155335.
18. Qi, Y., et al., *Synthesis of Quercetin Loaded Nanoparticles Based on Alginate for Pb(II) Adsorption in Aqueous Solution.* Nanoscale Research Letters, 2015. **10**(1): p. 408.
19. Rajesh, R. and Y. Dominic Ravichandran, *Development of a new carbon nanotube–alginate–hydroxyapatite tricomponent composite scaffold for application in bone tissue engineering.* International Journal of Nanomedicine, 2015. **10**(Suppl 1): p. 7-15.
20. K, J., et al., *Fabrication of cationized gelatin nanofibers by electrospinning for tissue regeneration.* RSC Advances, 2015. **5**(109): p. 89521-89530.
21. Sarker, B., et al., *Fabrication of alginate-gelatin crosslinked hydrogel microcapsules and evaluation of the microstructure and physico-chemical properties.* Journal of Materials Chemistry B, 2014. **2**(11): p. 1470-1482.
22. Rydén, L., et al., *Inflammatory cell response to ultra-thin amorphous and crystalline hydroxyapatite surfaces.* Journal of Materials Science: Materials in Medicine, 2016. **28**(1): p. 9.
23. Jiang, C., et al., *Crosslinked polyelectrolyte complex fiber membrane based on chitosan-sodium alginate by freeze-drying.* RSC Advances, 2014. **4**(78): p. 41551-41560.
24. Zhuang, C., F. Tao, and Y. Cui, *Anti-degradation gelatin films crosslinked by active ester based on cellulose.* RSC Advances, 2015. **5**(64): p. 52183-52193.
25. Stowers, R.S., S.C. Allen, and L.J. Suggs, *Dynamic phototuning of 3D hydrogel stiffness.* Proceedings of the National Academy of Sciences, 2015. **112**(7): p. 1953-1958.
26. Banerjee, A., et al., *The Influence of Hydrogel Modulus on the Proliferation and Differentiation of Encapsulated Neural Stem Cells.* Biomaterials, 2009. **30**(27): p. 4695-4699.
27. Huebsch, N., et al., *Matrix Elasticity of Void-Forming Hydrogels Controls Transplanted Stem Cell-Mediated Bone Formation.* Nature materials, 2015. **14**(12): p. 1269-1277.
28. Wu, Z., et al., *Bioprinting three-dimensional cell-laden tissue constructs with controllable degradation.* Scientific Reports, 2016. **6**: p. 24474.
29. Kim, Y.-S., et al., *Role of the epithelial–mesenchymal transition and its effects on embryonic stem cells.* Experimental & Molecular Medicine, 2014. **46**(8): p. e108.
30. Workman, M.J., et al., *Engineered human pluripotent-stem-cell-derived intestinal tissues with a functional enteric nervous system.* Nat Med, 2017. **23**(1): p. 49-59.
31. Monsel, A., et al., *Cell-based therapy for acute organ injury: preclinical evidence and ongoing clinical trials using mesenchymal stem cells.* Anesthesiology, 2014. **121**(5): p. 1099-121.
32. Nakatsu, H., et al., *Influence of mesenchymal stem cells on stomach tissue engineering using small intestinal submucosa.* J Tissue Eng Regen Med, 2015. **9**(3): p. 296-304.
33. Engevik, A.C., et al., *The Development of Spasmolytic Polypeptide/TFF2-Expressing Metaplasia (SPEM) During Gastric Repair Is Absent in the Aged Stomach.* Cellular and Molecular Gastroenterology and Hepatology, 2016. **2**(5): p. 605-624.
34. Lőrincz, A., et al., *PROGENITORS OF INTERSTITIAL CELLS OF CAJAL IN THE POSTNATAL MURINE STOMACH.* Gastroenterology, 2008. **134**(4): p. 1083-1093.
35. Torihashi, S., S.M. Ward, and K.M. Sanders, *Development of c-Kit-positive cells and the onset of electrical rhythmicity in murine small intestine.* Gastroenterology, 1997. **112**(1): p. 144-155.

36. Yanagida, H., et al., *Intestinal surgical resection disrupts electrical rhythmicity, neural responses, and interstitial cell networks.* Gastroenterology, 2004. **127**(6): p. 1748-1759.
37. Jiang, Y., et al., *Pluripotency of mesenchymal stem cells derived from adult marrow.* Nature, 2002. **418**(6893): p. 41-49.
38. Park, K.S., *Is this the era of interstitial cells of cajal transplantation?* Journal of neurogastroenterology and motility, 2014. **20**(3): p. 281.
39. McCann, C.J., et al., *Establishment of pacemaker activity in tissues allotransplanted with interstitial cells of Cajal.* Neurogastroenterology & Motility, 2013. **25**(6): p. e418-e428.
40. Joddar, B., S.A. Kumar, and A. Kumar, *A Contact-Based Method for Differentiation of Human Mesenchymal Stem Cells into an Endothelial Cell-Phenotype.* Cell Biochemistry and Biophysics, 2017. **Sep 23**: p. 1-9.
41. Sun, J. and H. Tan, *Alginate-Based Biomaterials for Regenerative Medicine Applications.* Materials, 2013. **6**(4): p. 1285.
42. Boskey, A., et al., *Osteopontin-hydroxyapatite interactions in vitro: inhibition of hydroxyapatite formation and growth in a gelatin-gel.* Bone and mineral, 1993. **22**(2): p. 147-159.
43. Gorgieva, S. and V. Kokol, *Collagen-vs. gelatine-based biomaterials and their biocompatibility: review and perspectives*. 2011: INTECH open access publisher Croatia.
44. Balakrishnan, B., et al., *Self-crosslinked oxidized alginate/gelatin hydrogel as injectable, adhesive biomimetic scaffolds for cartilage regeneration.* Acta Biomaterialia, 2014. **10**(8): p. 3650-3663.
45. Utech, S., et al., *Microfluidic generation of monodisperse, structurally homogeneous alginate microgels for cell encapsulation and 3D cell culture.* Advanced healthcare materials, 2015. **4**(11): p. 1628-1633.
46. Khademhosseini, A. and R. Langer, *Microengineered hydrogels for tissue engineering.* Biomaterials, 2007. **28**(34): p. 5087-5092.
47. Speer, A.L., et al., *Murine tissue-engineered stomach demonstrates epithelial differentiation.* J Surg Res, 2011. **171**(1): p. 6-14.